RAA 2014 Vol. **14** No. **4**, 390–400 doi: 10.1088/1674–4527/14/4/002
http://www.raa-journal.org *http://www.iop.org/journals/raa*

Research in Astronomy and Astrophysics

Pulsar timing residuals due to individual non-evolving gravitational wave sources *

Ming-Lei Tong[1,2], Cheng-Shi Zhao[1,2], Bao-Rong Yan[1,3], Ting-Gao Yang[1,2] and Yu-Ping Gao[1,2]

[1] National Time Service Center, Chinese Academy of Sciences, Xi'an 710600, China; *mltong@ntsc.ac.cn*
[2] Key Laboratory of Time and Frequency Primary Standards, Chinese Academy of Sciences, Xi'an 710600, China
[3] Key Laboratory of Precision Navigation and Timing Technology, Chinese Academy of Sciences, Xi'an 710600, China

Received 2013 October 2; accepted 2013 November 22

Abstract The pulsar timing residuals induced by gravitational waves from non-evolving single binary sources are affected by many parameters related to the relative positions of the pulsar and the gravitational wave sources. We will analyze the various effects due to different parameters. The standard deviations of the timing residuals will be calculated with a variable parameter fixing a set of other parameters. The orbits of the binary sources will be generally assumed to be elliptical. The influences of different eccentricities on the pulsar timing residuals will also be studied in detail. We find that the effects of the related parameters are quite different, and some of them display certain regularities.

Key words: gravitational waves: general — pulsars: general — binaries: general

1 INTRODUCTION

Gravitational waves (GWs) are believed to exist in the universe according to general relativity. The detection of GWs has been a very interesting field which has attracted much attention from many scientists. Even though indirect evidence of GW emission was provided by the observations of the binary pulsar B1913+16 (Hulse & Taylor 1974), no direct GW signals have been detected so far. However, many methods of direct detection of GWs have been proposed and tried for a long time. Various GW detectors were constructed or proposed for different frequencies, including ground-based interferometers, such as Advanced LIGO[1] and KAGRA (Somiya 2012) aiming at $10^2 - 10^3$ Hz; the space-based interferometers, such as eLISA[2] and ASTROD-GW (Ni 2013) aiming at $10^{-5} - 10^{-1}$ Hz; pulsar timing arrays (Sazhin 1978; Detweiler 1979; Foster & Backer 1990; Jenet et al. 2005; Hobbs et al. 2009) focused on $10^{-9} - 10^{-7}$ Hz, waveguides (Cruise 2000; Tong & Zhang 2008) in the range $10^{-6} - 10^{-8}$ Hz, Gaussian beams (Li et al. 2003; Tong et al. 2008) in GHz, and

∗ Supported by the National Natural Science Foundation of China

[1] *http://www.ligo.caltech.edu/advLIGO*
[2] *http://elisa-ngo.org*

even the anisotropies and polarizations of the cosmic microwave background radiation (Zaldarriaga & Seljak 1997; Kamionkowski et al. 1997) sensitive to 10^{-18} Hz.

With the improvement of radio telescopes, more and more pulsars have been found, and the measurement technique has become progressively more precise, which ensures pulsar timing arrays (PTAs) can be powerful in directly detecting GWs. The times-of-arrival (TOAs) of the pulses radiated from pulsars will fluctuate as GWs pass through the path between the pulsars and the Earth. As shown in Hellings & Downs (1983), a stochastic GW background can be detected by searching for correlations in the timing residuals of an array of millisecond pulsars spread over the sky. On the other hand, single sources of GWs are also important in observations from a pulsar timing array (Lee et al. 2011) or an individual pulsar (Jenet et al. 2004). Currently, there are several PTAs running, such as the Parkes Pulsar Timing Array (PPTA) (Manchester et al. 2013), the European Pulsar Timing Array (EPTA) (van Haasteren et al. 2011), the North American Nanohertz Observatory for Gravitational Waves (NANOGrav) (Demorest et al. 2013), and the International Pulsar Timing Array (IPTA) (Hobbs et al. 2010) formed by the aforesaid three PTAs. Moreover, the much more sensitive Five-hundred-meter Aperture Spherical Radio Telescope (FAST) (Nan et al. 2011) and Square Kilometre Array (SKA)[3] are also being planned.

There are chiefly three kinds of GW sources: continuous sources (Peters 1964), instantaneous sources (Thorne & Braginskii 1976) and the stochastic gravitational wave background (Grishchuk 1975; Starobinskiĭ 1979; Zhang et al. 2005; Tong 2013; Jaffe & Backer 2003; Damour & Vilenkin 2005). In the range of $\sim 10^{-9}-10^{-7}$ Hz, the major targets are GWs generated by supermassive black hole binaries (SMBHBs) (Jaffe & Backer 2003; Sesana & Vecchio 2010). As analyzed in Lee et al. (2011), a PTA is sensitive to nanohertz GWs from SMBHB systems with masses of $\sim 10^8-10^{10}M_\odot$ less than $10^5 - 10^6$ yr before the final merger. Binaries orbiting more than $\sim 10^3 - 10^4$ yr before the merger can be treated as non-evolving GW sources. The non-evolving SMBHBs are believed to be the dominant population, since they have lower masses and longer rest lifetimes. The pulsar timing residuals, defined as the difference between the observational TOAs and those predicted by the pulsar timing model, provide us with very important information. For example, one can fit the observational data using the least squares method to obtain the rotational frequency and its first derivative. As for GWs, the timing residuals of a pulsar timing array can be used to extract GW signals from various noises due to the correlations of the signals. On the other hand, GWs give rise to additional timing residuals, which will affect the precision of the pulsar timing standard. Hence, the studies of the timing residuals induced by GWs are important. In this paper, we fully analyze the timing residuals of an individual pulsar induced by single non-evolving GW sources of SMBHBs localized in various positions in the international celestial reference frame. They are related to many parameters. We will discuss the effects of all these respective parameters on the timing residuals and their standard deviations. Following the discussions in references (Wahlquist 1987; Tong et al. 2013), we generally assume the orbits of the SMBHBs are elliptical, i.e., the eccentricities will be nonzero. For example, one of the best-known candidates of an SMBHB system emitting GWs with frequencies detectable by pulsar timing is in blazar OJ 287 (Sillanpaa et al. 1996), with an orbital eccentricity of $e \sim 0.7$ (Sundelius et al. 1997; Zhang et al. 2013). Moreover, if we consider the existence of circumbinary gaseous disks in which the SMBHBs are embedded, the binary orbits are usually eccentric (Roedig et al. 2011). However, we will not consider the transfer of angular momentum between the SMBHBs and their self-gravitating disks. The effect of different values of the eccentricities on the standard deviations of the timing residuals will also be studied. Throughout this paper, we use units in which $c = G = 1$.

In Section 2, we show the analytical solution of GWs from an SMBHB with a general elliptical orbit. Section 3 describes how a singe GW induces pulsar timing residuals. Various effects due to

[3] *http://www.skatelescope.org*

different parameters on the standard deviations of the pulsar timing residuals will be analyzed in Section 4. Section 5 provides some conclusions and discussion.

2 THE ANALYTICAL SOLUTION OF GWS FROM AN SMBHB WITH AN ELLIPTICAL ORBIT

First of all, we simply describe the derivations of the GW solution from a binary star system with an elliptical orbit by following Wahlquist (1987). The usual equation for the orbital ellipse describing relative motion is given by

$$r = \frac{a(1-e^2)}{1+e\cos(\theta-\theta_{\rm p})}, \tag{1}$$

where r is the separation of the binary components, a is the semi-major axis and $\theta_{\rm p}$ is the value of θ at the periastron. Since different values of $\theta_{\rm p}$ correspond to different choices of the initial time, we concretely set $\theta_{\rm p} = 180^\circ$ without losing generality in the following. The orbital period of the binary system is

$$P = \left(\frac{4\pi^2 a^3}{M}\right)^{1/2}, \tag{2}$$

where M is the total mass of the binary system. According to the differential equation for Keplerian motion (Wahlquist 1987)

$$\dot{\theta} = (2\pi/P)(1-e^2)^{-3/2}[1+e\cos(\theta-\theta_{\rm p})]^2. \tag{3}$$

Integrating the above equation, one has the relation between t and θ, which is shown in figure 1 in Tong et al. (2013).

For observations, one needs to obtain the solution of GWs described in the frame where the origin is located at the solar system barycenter (SSB). Thus, let us define the problem in terms of the international celestial reference frame (ICRF) whose origin is the SSB. Let $\{\hat{i},\hat{j},\hat{k}\}$ be the base vectors of the ICRF. Then the unit vector of a GW source is

$$\hat{d} = \cos\delta(\cos\alpha\,\hat{i} + \sin\alpha\,\hat{j}) + \sin\delta\,\hat{k}, \tag{4}$$

where α and δ are the right ascension and declination of the binary source, respectively. Define orthonormal vectors on the celestial sphere by (Wahlquist 1987)

$$\hat{\alpha} \equiv -\sin\alpha\,\hat{i} + \cos\alpha\,\hat{j}, \tag{5}$$

$$\hat{\delta} \equiv -\sin\delta(\cos\alpha\,\hat{i} + \sin\alpha\,\hat{j}) + \cos\delta\,\hat{k}. \tag{6}$$

Moreover, let $\hat{u}$ be a unit vector which lies in the orbital plane of the binary along the line of nodes, which is defined to be the intersection of the orbital plane with the tangent plane of the sky. Then $\hat{u}\cdot\hat{d} = 0$, and one can write

$$\hat{u} = \cos\phi\,\hat{\alpha} + \sin\phi\,\hat{\delta}, \tag{7}$$

where ϕ defines the orientation of the line of nodes in the sky. In the linearized theory of general relativity, the metric perturbation is given to lowest order by the second-time derivative of the quadrupole moment of the source (Misner et al. 1973)

$$h_{ab}^{\rm TT}(t) = \frac{2}{R}\ddot{Q}_{ab}^{\rm TT}(t-d), \tag{8}$$

where d is the distance to the GW source, $h_{ab}^{\rm TT}$ describes the waveform of GWs in the transverse-traceless (TT) gauge and $Q_{ab}^{\rm TT}$ is the quadrupole moment of the source evaluated in the retarded time $t-d$. For a GW traveling in a definite direction Ω, the waveform of GWs is usually written as

$$h_{ab}^{\rm TT}(t,\hat{\Omega}) = h_+(t)\epsilon_{ab}^+(\hat{\Omega}) + h_\times(t)\epsilon_{ab}^\times(\hat{\Omega}), \tag{9}$$

where $\hat{\Omega} = -\hat{d}$ is the unit vector pointing from the GW source to the SSB. The polarization tensors are (Lee et al. 2011; Ellis et al. 2012)

$$\epsilon^{+}_{ab}(\hat{\Omega}) = \begin{pmatrix} \sin^2\alpha - \cos^2\alpha\sin^2\delta & -\sin\alpha\cos\alpha(\sin^2\delta+1) & \cos\alpha\sin\delta\cos\delta \\ -\sin\alpha\cos\alpha(\sin^2\delta+1) & \cos^2\alpha - \sin^2\alpha\sin^2\delta & \sin\alpha\sin\delta\cos\delta \\ \cos\alpha\sin\delta\cos\delta & \sin\alpha\sin\delta\cos\delta & -\cos^2\delta \end{pmatrix}, \tag{10}$$

$$\epsilon^{\times}_{ab}(\hat{\Omega}) = \begin{pmatrix} \sin(2\alpha)\sin\delta & -\cos(2\alpha)\sin\delta & -\sin\alpha\cos\delta \\ -\cos(2\alpha)\sin\delta & -\sin(2\alpha)\sin\delta & \cos\alpha\cos\delta \\ -\sin\alpha\cos\delta & \cos\alpha\cos\delta & 0 \end{pmatrix}. \tag{11}$$

For an SMBHB with an elliptical orbit, the polarization amplitudes of the emitting GWs are (Wahlquist 1987)

$$h_{+}(\theta) = H\Big\{\cos(2\phi)[A_0 + eA_1 + e^2A_2] - \sin(2\phi)[B_0 + eB_1 + e^2B_2]\Big\}, \tag{12}$$

$$h_{\times}(\theta) = H\Big\{\sin(2\phi)[A_0 + eA_1 + e^2A_2] + \cos(2\phi)[B_0 + eB_1 + e^2B_2]\Big\}, \tag{13}$$

with ϕ being the orientation of the line of nodes, which is defined to be the intersection of the orbital plane with the tangent plane of the sky. The parameters in Equations (12) and (13) are

$$\begin{aligned} H &\equiv \tfrac{2^{8/3}\pi^{2/3}M_c^{5/3}(1+z)^{5/3}}{(1-e^2)P_{\rm obs}^{2/3}D_L}, \\ A_0 &= -\tfrac{1}{2}[1+\cos^2(\iota)]\cos(2\theta), \\ B_0 &= -\cos(\iota)\sin(2\theta), \\ A_1 &= -\tfrac{1}{4}\sin^2(\iota)\cos\theta + \tfrac{1}{8}[1+\cos^2(\iota)][5\cos\theta + \cos(3\theta)], \\ B_1 &= \tfrac{1}{4}\cos(\iota)[5\sin(\theta) + \sin(3\theta)], \\ A_2 &= \tfrac{1}{4}\sin^2(\iota) - \tfrac{1}{4}[1+\cos^2(\iota)], \\ B_2 &= 0. \end{aligned} \tag{14}$$

Note that, compared to those shown in Wahlquist (1987), in Equation (14) we have chosen $\theta_n = 0$, the value of θ at the line of nodes. Moreover, $M_c = \mu^{3/5}M^{2/5}$ is the chirp mass with μ being the reduced mass of the binary system. The appearance of the factor $(1+z)^{5/3}$ included in the expression of H is due to the effect of cosmological redshift. ι is the angle of inclination of the orbital plane with respect to the tangent plane of the sky, $P_{\rm obs} = P(1+z)$ is the observational period of the binary and D_L is the luminosity distance from the binary system to the SSB. In the standard cosmological model, the luminosity distance is given by

$$D_L = \frac{1+z}{H_0}\int_0^z \frac{dz'}{\sqrt{\Omega_\Lambda + \Omega_m(1+z')^3}}, \tag{15}$$

where H_0 is the Hubble constant, z is the cosmological redshift and Ω_Λ and Ω_m are the density contrast of dark energy and matter respectively. From the observations of WMAP covering nine years (Hinshaw et al. 2013), one has $H_0 = 69.7\,\mathrm{km\ s^{-1}\ Mpc^{-1}}$, $\Omega_\Lambda = 0.72$ and $\Omega_m = 0.28$. For the particular case of $e = 0$, Equations (12) and (13) reduce to (Lee et al. 2011)

$$h_{+}(t) = h_0\left[\cos\iota\sin(2\phi)\sin(\omega_g t) - \frac{1}{2}(1+\cos^2\iota)\cos(2\phi)\cos(\omega_g t)\right], \tag{16}$$

$$h_{\times}(t) = -h_0\left[\cos\iota\cos(2\phi)\sin(\omega_g t) + \frac{1}{2}(1+\cos^2\iota)\sin(2\phi)\cos(\omega_g t)\right], \tag{17}$$

where $h_0 = 2^{4/3} {M_c}^{5/3} \omega_g^{2/3} D_L^{-1}(1+z)$ with $\omega_g = 4\pi/P$ being the angular frequency of the radiated GWs at the source. It is worth pointing out that the time t in Equations (16) and (17) stands for the timescale around the GW source. Alternatively, one can rewrite Equations (16) and (17) using the time at observer t'. Due to the effect of cosmological redshift, one has $t' = t(1+z)$ if the zero points of t and t' are chosen to be the same. One the other hand, the intrinsic frequency of the GWs will suffer from a redshift, that is, $\omega_g^{(\rm obs)} = \omega_g/(1+z)$, where $\omega_g^{(\rm obs)}$ is the observed angular frequency of GWs. Thus, one has $\omega_g t \equiv \omega_g^{(\rm obs)} t'$, and h_0 can be expressed as

$$h_0 = 2^{4/3} {M_c}^{5/3} (\omega_g^{(\rm obs)})^{2/3} D_L^{-1} (1+z)^{5/3} \,.$$

3 THE PULSAR TIMING RESIDUALS INDUCED BY A SINGLE GW

The GW will cause a fractional shift in frequency, ν, which can be defined by a redshift (Demorest et al. 2013; Ellis et al. 2012; Anholm et al. 2009)

$$z(t, \hat{\Omega}) \equiv \frac{\delta\nu(t, \hat{\Omega})}{\nu} = -\frac{1}{2} \frac{\hat{n}^a \hat{n}^b}{1 + \hat{n} \cdot \hat{\Omega}} \epsilon_{ab}^A(\hat{\Omega}) \Delta h_A(t), \tag{18}$$

where

$$\Delta h_A(t) = h_A(t_{\rm e}) - h_A(t_{\rm p}). \tag{19}$$

Here A denotes "$+, \times$" and the standard Einstein summation convention is used. $t_{\rm e}$ and $t_{\rm p}$ are the time at which the GW passes the Earth and pulsar, respectively. Henceforth, we will drop the subscript "e" denoting the time for the Earth unless otherwise noted. The unit vector, $\hat{n}$, pointing from the SSB to the pulsar is explicitly written as

$$\hat{n} = \cos\delta_{\rm p}[\cos\alpha_{\rm p}\hat{i} + \sin\alpha_{\rm p}\hat{j}] + \sin\delta_{\rm p}\hat{k}, \tag{20}$$

where $\alpha_{\rm p}$ and $\delta_{\rm p}$ are the right ascension and declination of the pulsar, respectively. From geometry one has (Ellis et al. 2012; Anholm et al. 2009)

$$t_{\rm p} = t - D_{\rm p}(1 - \cos\eta), \tag{21}$$

where $D_{\rm p}$ is the distance to the pulsar and $\cos\eta = -\hat{n} \cdot \hat{\Omega} = \hat{n} \cdot \hat{d}$ with η being the angle between the direction of the pulsar and that of the GW source. Combining Equations (10)–(18), we obtain

$$z(t, \hat{\Omega}) = -\frac{1}{2}(1 + \cos\eta)\Big\{ \cos(2\lambda)\Big[h_+(t) - h_+(t_{\rm p})\Big] + \sin(2\lambda)\Big[h_\times(t) - h_\times(t_{\rm p})\Big]\Big\}, \tag{22}$$

where $\cos\eta = \sin\delta_{\rm p}\sin\delta + \cos\delta_{\rm p}\cos\delta\cos(\alpha - \alpha_{\rm p})$, and λ is defined as (Wahlquist 1987)

$$\tan\lambda \equiv \frac{\hat{n} \cdot \hat{\delta}}{\hat{n} \cdot \hat{\alpha}} = \frac{\cos\delta_{\rm p}\sin\delta\cos(\alpha - \alpha_{\rm p}) - \sin\delta_{\rm p}\cos\delta}{\cos\delta_{\rm p}\sin(\alpha - \alpha_{\rm p})}, \tag{23}$$

where Equations (5), (6) and (20) are used. It can be found from Equation (22) that the frequency of the pulses from the pulsar will suffer no shift from the GW for $\eta = 0^\circ$ and $\eta = 180^\circ$ by taking into account Equation (21).

The pulsar timing residuals induced by GWs can be computed by integrating the redshift given in Equation (22) over the observer's local time (Hobbs et al. 2009; Lee et al. 2011; Ellis et al. 2012; Anholm et al. 2009)

$$R(t, \hat{\Omega}) = \int_0^t z(t', \hat{\Omega}) dt'. \tag{24}$$

For the particular case of $e = 0$, one has the analytical expressions of the timing residuals as follows,

$$\begin{aligned} R(t,\hat{\Omega}) &= \frac{h_0 \sin(\Delta\Phi/2)}{2\omega_g(1-\cos\eta)}\Big\{\Big[C_+\cos(2\phi)+C_\times\sin(2\phi)\Big](1+\cos^2\iota)\cos(\omega_g t-\Delta\Phi/2) \\ &\quad +2\Big[C_\times\cos(2\phi)-C_+\sin(2\phi)\Big]\cos\iota\sin(\omega_g t-\Delta\Phi/2)\Big\}, \end{aligned}$$

where C_+, $C_\times$ and $\Delta\Phi$ depend on the geometrical configuration of the pulsar and GW source as described by

$$\begin{aligned} C_+ &= \tfrac{1}{4}\cos^2\delta_{\rm p}\Big\{2\cos^2\delta+[\cos(2\delta)-3]\cos[2(\alpha_{\rm p}-\alpha)]\Big\}-\cos^2\delta\sin^2\delta_{\rm p} \\ &\quad +\cos\delta_{\rm p}\cos(\alpha_{\rm p}-\alpha)\sin\delta_{\rm p}\sin(2\delta) \end{aligned}$$

$$C_\times = \cos\delta\sin(2\delta_{\rm p})\sin(\alpha_{\rm p}-\alpha)-\sin\delta\cos^2\delta_{\rm p}\sin[2(\alpha_{\rm p}-\alpha)], \tag{25}$$

$$\Delta\Phi = \omega_g D_{\rm p}(1-\cos\eta). \tag{26}$$

It is also interesting to calculate the standard deviation of the timing residuals for a definite direction of GWs, σ_R, which is defined as (Hobbs et al. 2009)

$$\sigma_R = \left[\frac{1}{T}\int_0^T R^2(t)dt-\left(\frac{1}{T}\int_0^T R(t)dt\right)^2\right]^{1/2}, \tag{27}$$

where T can be chosen as the period P due to the periodicity of $R(t)$.

4 THE PROPERTIES OF THE TIMING RESIDUALS AFFECTED BY ALL THE RELATED PARAMETERS

As can be seen from the above, the pulsar timing residuals are related to many parameters, such as e, ϕ, ι, λ and η. The different properties of $R(t)$ and σ_R due to different values of e with a constant H have been studied preliminarily in Tong et al. (2013). In this section, we analyze the properties of $R(t)$ and σ_R induced by all the related parameters. SMBHBs are the ideal GW sources detected by pulsar timing arrays (Hobbs et al. 2009; Sesana & Vecchio 2010), whose response frequencies are in the range $\sim 10^{-9}-10^{-7}$ Hz. Hence we can set the observed orbital period of an SMBHB to be $P_{\rm obs} = 10^9$ s for instance, since the frequencies of the GWs from an SMBHB with an elliptical orbit are a few or tens times the orbital frequency of the binary system (Wahlquist 1987; Maggiore 2007). With fixed values of all the related parameters, one can calculate $R(t)$ and σ_R. As shown in Tong et al. (2013), $R(t)$ presents quite different behaviors for different values of e. Thus, one can infer that $R(t)$ will exhibit complexities for different values of various parameters. We will not illustrate the properties of $R(t)$ in this paper but instead focus on the more essential σ_R. Below, for illustration, we assume $H = 10^{-15}$, which is below the upper limit given in Yardley et al. (2010), and take $e = 0.3$ for instance, except for the additional analysis on the different values of e.

4.1 The Effects of λ and η

First of all, we fix $\phi = \iota = 0$ following Wahlquist (1987) and Tong et al. (2013). The waveforms of the polarization amplitudes $h_+(t)$ and $h_\times(t)$ for different e were shown in Wahlquist (1987). Moreover, we always set $D_{\rm p} = 157$ pc, the distance from the SSB to PSR J0437–4715 (Verbiest et al. 2008). Thus, there are only two free parameters, λ and η. Firstly, set $\eta = 60^\circ$, and we get $\sigma_R = 33$ ns for all the values of $\lambda \in [0, 360^\circ]$. That is, σ_R has nothing to do with λ. Therefore, we will set $\lambda = 0$ in the following without losing generality. Secondly, we discuss the influences of η.

In Figure 1, we plot σ_R versus η. One can see that σ_R has a decreasing trend with η and decays to zero at $\eta = 180^\circ$. Therefore, if the pulsar and the GW source are almost in the same direction as the observer, signals from the pulsar will be distinctly affected by GWs. However, one should note that $\sigma_R = 0$ for $\eta = 0$ due to Equation (21).

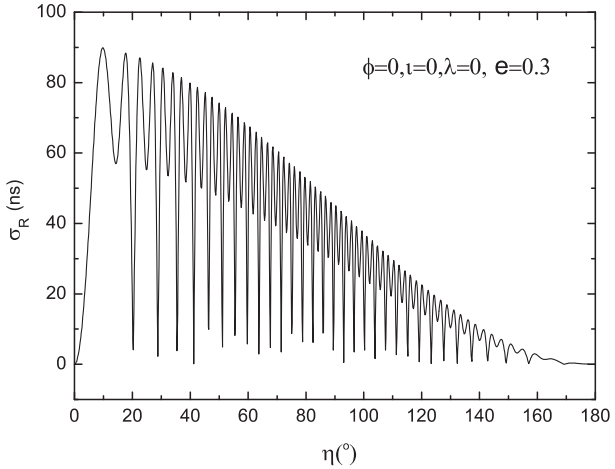

Fig. 1 The variety of values for σ_R as a function of η for $e = 0.3$ and $H = 10^{-15}$.

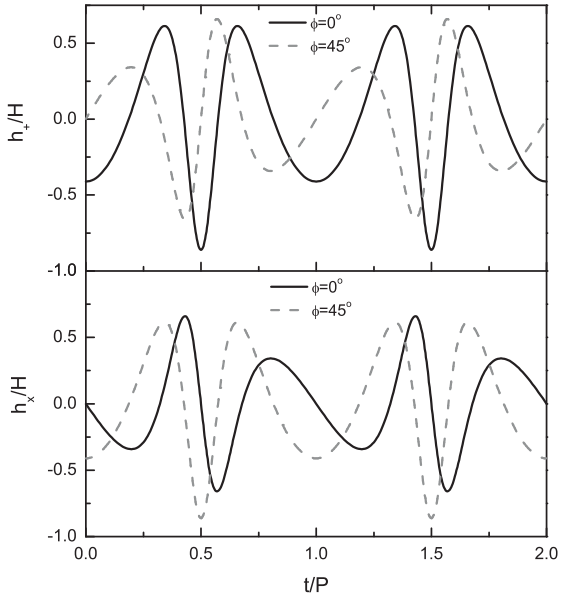

Fig. 2 $h_+(t)$ and $h_\times(t)$ normalized by H for $\phi = 0$ and $\phi = 45°$, respectively, with $e = 0.3$ and $\iota = 60°$.

4.2 The Effects of ϕ and ι

For a full analysis, now we discuss the influences of different values of ϕ and ι on σ_R. As can be seen in Equations (12) and (14), different values of ϕ and ι will change the waveforms of $h_+(t)$ and $h_\times(t)$.

Figure 2 shows $h_+(t)$ and $h_\times(t)$ for $\phi = 0$ and $\phi = 45°$, respectively, for a fixed $\iota = 60°$. Similarly, Figure 3 shows $h_+(t)$ and $h_\times(t)$ for $\iota = 0$ and $\iota = 90°$, respectively, for a fixed $\phi = 30°$.

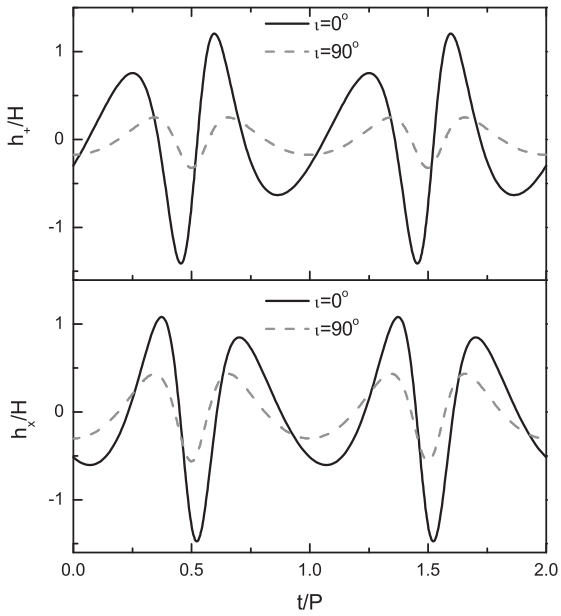

Fig. 3 $h_+(t)$ and $h_\times(t)$ normalized by H for $\iota = 0$ and $\iota = 90^\circ$, respectively, with $e = 0.3$ and $\phi = 30^\circ$.

Using the concrete forms of $h_+(t)$ and $h_\times(t)$, we can calculate the corresponding σ_R with the help of Equation (27). Setting $\eta = 60^\circ$, the resulting σ_R versus ϕ with fixed $\iota = 60^\circ$ is shown in Figure 4. Similarly, the resulting σ_R versus ι with fixed $\phi = 30^\circ$ is shown in Figure 5. From Figure 4, it can be found that the maximal change in σ_R is about 4.1 ns due to different ϕ. On the other hand, the maximal change in σ_R due to different ι is about 24.7 ns as shown in Figure 5. Therefore, ι affects σ_R more distinctly than ϕ does. This is implied in Figures 2 and 3, which show that ι affects the polarization amplitudes of GWs more dramatically than ϕ does. Note that σ_R is proportional to the polarization amplitudes of GWs, and in turn, H. Moreover, σ_R shows periodicity as a function of ϕ with a period of $\pi/2$, and σ_R is symmetrical relative to $\iota = 90^\circ$ where σ_R has a minimal value. Hence, the SMBHB with an orbital plane perpendicular to the line of sight of the observer will contribute to the timing residuals the least.

4.3 The Effect of e

The effect of different e on the timing residuals has been studied in Tong et al. (2013), for a fixed value of H. Here, we focus on the effect of e on the standard deviation σ_R. First of all, the waveforms of the polarization amplitudes are quite different for different e with $\phi = \iota = 0$, as shown in Wahlquist (1987). When calculating σ_R, we consider two cases with different values of H. Firstly, we fix $H = 10^{-15}$. Secondly, we fix $H' \equiv H|_{e=0} = \frac{2^{8/3}\pi^{2/3}M_c^{5/3}(1+z)^{5/3}}{P_{\rm obs}^{2/3}D_L} = 10^{-15}$. For a concrete set of parameters $\phi = 30^\circ$, $\iota = 60^\circ$, $\lambda = 0$ and $\eta = 45^\circ$, the resulting σ_R as a function of e for the two cases is listed in Tables 1 and 2, respectively. Furthermore, interpolation curves of the data in Tables 1 and 2 are plotted together in Figure 6. One can clearly see that, for a definite set of parameters, σ_R distinctly decreases with larger values of e in the case of $H = 10^{-15}$, however, the change in σ_R is relatively small and levels off for $e \geq 0.6$ in the case of $H' = 10^{-15}$. The

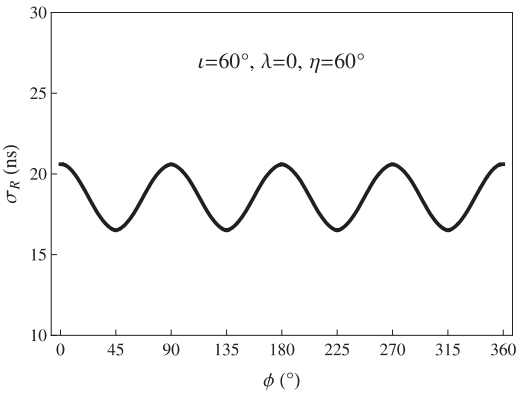

Fig. 4 The variety of values for σ_R as a function of ϕ for $e = 0.3$.

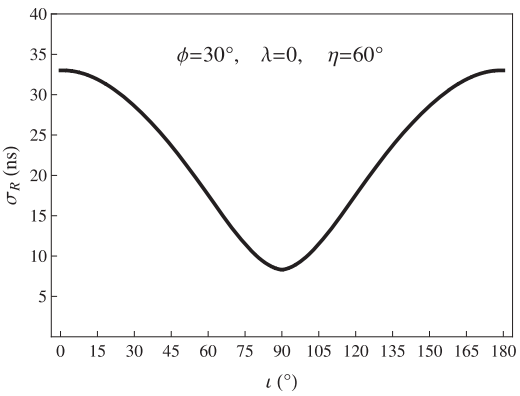

Fig. 5 The variety of values for σ_R as a function of ι for $e = 0.3$.

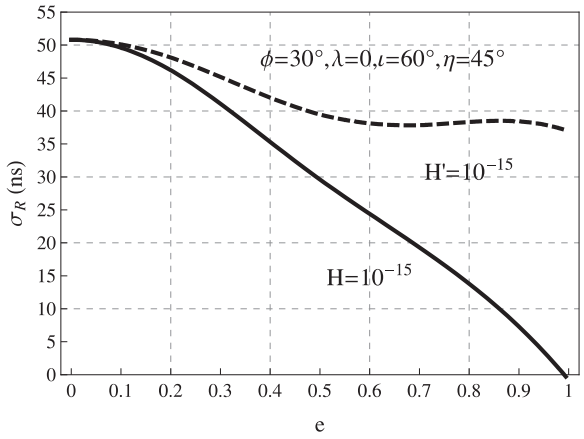

Fig. 6 The variety of values for σ_R as a function of e for $H = 10^{-15}$ and $H' = 10^{-15}$.

two cases give rise to quite different results, especially for larger values of e. Therefore, when doing simulations of GW sources, one should clarify the assumptions since a discrepancy exists between the two cases.

Table 1 σ_R for different e with $H = 10^{-15}$. The set of parameters were chosen as $\phi = 30°$, $\iota = 60°$, $\lambda = 0$ and $\eta = 45°$.

e	0	0.1	0.2	0.3	0.4	0.5	0.6	0.7	0.8	0.9
σ_R (ns)	50.8	49.6	46.2	41.1	35.3	29.6	24.4	19.3	13.8	7.3

Table 2 σ_R for different e with $H' = 10^{-15}$. The set of parameters were chosen exactly the same as Table 1.

e	0	0.1	0.2	0.3	0.4	0.5	0.6	0.7	0.8	0.9
σ_R (ns)	50.8	50.1	48.1	45.2	42.0	39.5	38.1	37.8	38.3	38.4

5 CONCLUSIONS AND DISCUSSION

The pulsar timing residuals induced by GWs from single sources are related to many parameters. We have analyzed the effects of various parameters on the timing residuals $R(t)$ and their standard deviations σ_R. Among all the related parameters, different λ will not change σ_R. Generally speaking, a larger η leads to a smaller σ_R except for $\eta = 0$. On the other hand, σ_R shows periodicity as a function of ϕ with a period equalling $\pi/2$, and σ_R is symmetrical relative to $\iota = 90^\circ$, where σ_R has a minimum. Moreover, for other definite values of parameters, σ_R decreases with larger e in the case of fixed value $H = 10^{-15}$, however, σ_R will not change so much in the case of $H' \equiv H|_{e=0} = 10^{-15}$. It is worth noting that the timing residuals and the standard deviations are both proportional to the polarization amplitudes, and in turn H. By comparison, the parameters η, ι and e evidently affect σ_R. If one wants to detect single GW sources, due to a lack of essential information about the sources, the sensitivities of these parameters analyzed above could give a hint on how to reduce the possible parameter space. On the other hand, for the study of a pulsar timing standard, GWs are one kind of timing noise. Knowing how a strong GW source like the SMBHB in the blazar OJ 287 (Sillanpaa et al. 1996) affects the timing signals from pulsars is very important for constructing a pulsar timing standard.

Note that all the results are based on non-evolving single sources. Evolving sources, especially SMBHBs in the merging phase, will radiate much stronger GWs, which are easier to detect. So, the pulsar timing residuals induced by GWs from the merging of SMBHBs are worth studying elsewhere. In this case, a single GW source is instantaneous rather than continuous, and the eccentricity will decay almost to zero.

Acknowledgements This work was supported by the National Natural Science Foundation of China (Grant No. 11103024 and 11373028) and the program of the West Light Foundation of the Chinese Academy of Sciences.

References

Anholm, M., Ballmer, S., Creighton, J. D. E., Price, L. R., & Siemens, X. 2009, Phys. Rev. D, 79, 084030
Cruise, A. M. 2000, Classical and Quantum Gravity, 17, 2525
Damour, T., & Vilenkin, A. 2005, Phys. Rev. D, 71, 063510
Demorest, P. B., Ferdman, R. D., Gonzalez, M. E., et al. 2013, ApJ, 762, 94
Detweiler, S. 1979, ApJ, 234, 1100
Ellis, J. A., Jenet, F. A., & McLaughlin, M. A. 2012, ApJ, 753, 96
Foster, R. S., & Backer, D. C. 1990, ApJ, 361, 300
Grishchuk, L. P. 1975, Soviet Journal of Experimental and Theoretical Physics, 40, 409
Hellings, R. W., & Downs, G. S. 1983, ApJ, 265, L39
Hinshaw, G., Larson, D., Komatsu, E., et al. 2013, ApJS, 208, 19
Hobbs, G., Jenet, F., Lee, K. J., et al. 2009, MNRAS, 394, 1945
Hobbs, G., Archibald, A., Arzoumanian, Z., et al. 2010, Classical and Quantum Gravity, 27, 084013
Hulse, R. A., & Taylor, J. H. 1974, ApJ, 191, L59
Jaffe, A. H., & Backer, D. C. 2003, ApJ, 583, 616
Jenet, F. A., Hobbs, G. B., Lee, K. J., & Manchester, R. N. 2005, ApJ, 625, L123
Jenet, F. A., Lommen, A., Larson, S. L., & Wen, L. 2004, ApJ, 606, 799
Kamionkowski, M., Kosowsky, A., & Stebbins, A. 1997, Phys. Rev. D, 55, 7368
Lee, K. J., Wex, N., Kramer, M., et al. 2011, MNRAS, 414, 3251
Li, F.-Y., Tang, M.-X., & Shi, D.-P. 2003, Phys. Rev. D, 67, 104008
Maggiore, M. 2007, Gravitational Waves: Volume 1: Theory and Experiments, 1 (Oxford: Oxford Univ. Press)
Manchester, R. N., Hobbs, G., Bailes, M., et al. 2013, PASA, 30, e017

Misner, C. W., Thorne, K. S., & Wheeler, J. A. 1973, Gravitation (San Francisco: W. H. Freeman and Co.)
Nan, R., Li, D., Jin, C., et al. 2011, International Journal of Modern Physics D, 20, 989
Ni, W.-T. 2013, International Journal of Modern Physics D, 22, 1341004
Peters, P. C. 1964, Physical Review, 136, B1224
Roedig, C., Dotti, M., Sesana, A., Cuadra, J., & Colpi, M. 2011, MNRAS, 415, 3033
Sazhin, M. V. 1978, Soviet Ast., 22, 36
Sesana, A., & Vecchio, A. 2010, Classical and Quantum Gravity, 27, 084016
Sillanpaa, A., Takalo, L. O., Pursimo, T., et al. 1996, A&A, 305, L17
Somiya, K. 2012, Classical and Quantum Gravity, 29, 124007
Starobinskiĭ, A. A. 1979, Soviet Journal of Experimental and Theoretical Physics Letters, 30, 682
Sundelius, B., Wahde, M., Lehto, H. J., & Valtonen, M. J. 1997, ApJ, 484, 180
Thorne, K. S., & Braginskii, V. B. 1976, ApJ, 204, L1
Tong, M. 2013, Classical and Quantum Gravity, 30, 055013
Tong, M.-L., Yan, B.-R., Zhao, C.-S., et al. 2013, Chinese Physics Letters, 30, 100402
Tong, M.-L., & Zhang, Y. 2008, ChJAA (Chin. J. Astron. Astrophys.), 8, 314
Tong, M. L., Zhang, Y., & Li, F. Y. 2008, Phys. Rev. D, 78, 024041
van Haasteren, R., Levin, Y., Janssen, G. H., et al. 2011, MNRAS, 414, 3117
Verbiest, J. P. W., Bailes, M., van Straten, W., et al. 2008, ApJ, 679, 675
Wahlquist, H. 1987, General Relativity and Gravitation, 19, 1101
Yardley, D. R. B., Hobbs, G. B., Jenet, F. A., et al. 2010, MNRAS, 407, 669
Zaldarriaga, M., & Seljak, U. 1997, Phys. Rev. D, 55, 1830
Zhang, Y., Wu, S. G., & Zhao, W. 2013, arXiv:1305.1122
Zhang, Y., Yuan, Y., Zhao, W., & Chen, Y.-T. 2005, Classical and Quantum Gravity, 22, 1383